Proceedings of the Combustion Institute, Volume 29, 2002/pp. 1411–1417

IMPLEMENTATION OF COMBUSTION CHEMISTRY BY *IN SITU* ADAPTIVE TABULATION OF RATE-CONTROLLED CONSTRAINED EQUILIBRIUM MANIFOLDS

QING TANG AND STEPHEN B. POPE
Sibley School of Mechanical and Aerospace Engineering
Cornell University
Ithaca, NY 14853-7501, USA

A general methodology called *in situ* adaptive tabulation-rate-controlled constrained equilibrium (ISAT-RCCE) is developed to treat detailed chemistry in turbulent combustion calculations. This method combines dimension reduction and tabulation and can be implemented in a single computer program, which is independent of the detailed mechanism and of the level of reduction selected. The dimension reduction of a detailed mechanism is achieved by the RCCE approach, which is based on the maximum entropy principle of thermodynamics; and the tabulation is performed *in situ* during the combustion calculations and is made in the low-dimensional constraint subspace. This method is particularly attractive for very large kinetic mechanisms (e.g., including thousands of species) because the constrained equilibrium state depends on only a small number of constraints (or constraint potentials) which form the constraint subspace. Moreover, the unique and continuous maximum-entropy manifold determined by the RCCE assumption is well suited to the ISAT algorithm—an efficient computational technique for the implementation of combustion chemistry. Test calculations are performed for non-premixed methane/air combustion in a statistically homogeneous turbulent reactor, using a detailed kinetic mechanism with 31 species and 175 reactions. A direct approach of numerically integrating the full reaction equations (32-dimensional) is performed and the result is taken as the exact solution. The ISAT-RCCE calculations based on 10- to 16-dimensional constraint subspaces show good agreement with the accurate solution, and the accuracy of the results from the 16-dimensional ISAT-RCCE calculation is comparable to that of a reference calculation using ISAT and a 17-dimensional augmented reduced mechanism (derived from the same detailed mechanism). A speed-up factor of about 500 is obtained for the ISAT-RCCE calculation compared to the direct integration approach, which demonstrates the high efficiency of the new method.

Introduction

Combustion chemistry is highly complex: a realistic description of even the simplest hydrocarbon oxidation involves tens of species undergoing hundreds of reactions, and the time scales vary over many orders of magnitude. Unfortunately, despite the rapid advances in computational power, for most practical turbulent combustion phenomena, it remains impracticable to make direct numerical simulations (or even model calculations) including such detailed chemistry. This fact has provided the motivation in the past two decades for the development of methodologies to reduce the computational cost of solving the equations governing the complex chemical system.

Among the available techniques, two of the most frequently used in the literature are dimension reduction and storage/retrieval. From a geometric point of view, dimension reduction methods represent the chemical kinetics on a low-dimensional manifold in composition space. These manifolds are identified via, for example, quasi-steady-state assumptions (QSSA) [1,2], the maximum entropy principle of thermodynamics (rate-controlled constrained equilibrium, RCCE) [3], or a dynamical systems approach (ILDM) [4]. On the other hand, storage/retrieval is aimed at the computationally efficient implementation of the chemical mechanisms (full or reduced) in combustion calculations. There are many methods that fall in this category, such as the tabulation methods structured look-up table (LUT) [5] and *in situ* adaptive tabulation (ISAT) [6]. Others include those that rely on orthogonal polynomials (repromodeling [7], PRISM [8]), artificial neural networks [9], and high-dimension model representations (HDMR) [10].

The application of structured LUT is restricted to systems of quite low dimension (e.g., $n = 2$ or 3), because the table storage and retrieval work increase exponentially with n. The ISAT scheme creates an unstructured look-up table dynamically as the reactive flow calculation is performed. For a given combustion problem, with the chemistry described at different levels (characterized by the dimension n),

TABLE 1
Attributes of different dimension reduction methodologies

	ILDM	QSSA	RCCE
Identification of fast directions	Automatic/local	Specified/global	Specified/global
Uniqueness and continuity of manifold	Not always	Not always	Guaranteed
Inertial manifold	No	No	No
Second Law of thermodynamics	?	?	Satisfied
Ease of parametrization	Difficult	Simple	Simple
Size of nonlinear equation system	$n - n_r$	$n - n_r$	n_r

both the storage and the retrieval work in ISAT increase as n^2. This feature enables ISAT to implement moderate-size chemical mechanisms efficiently and thus capture the combustion characteristics in more detail. Successful applications of ISAT to realistic turbulent combustion modeling have been reported recently [11–13], where two augmented reduced mechanisms [14] comprising about 20 species are employed in the calculations. This approach is referred to as ISAT-QSSA.

In the ISAT-QSSA approach, the reduction (QSSA) and tabulation (ISAT) are separate and are implemented using separate computer programs. Different QSSA schemes must be developed for different fuels and for different detailed mechanisms. The objective of the present work is to develop a general, combined reduction/tabulation methodology. An example of the application of this type of methodology is as follows: a detailed 100-species mechanism is provided; the reactive flow calculation is performed in terms of 10 reduced variables; and the reduction/tabulation methodology determines and tabulates (*in situ*) the necessary information about the 10-dimensional reduced system based on the 100-species detailed mechanism. This methodology can be implemented in a single computer program, which is independent of the detailed mechanism and of the level of reduction selected.

In this paper, we report the development of such a combined methodology (ISAT-RCCE), in which the reduction is based on the RCCE approach, and the tabulation is performed by ISAT.

The three reduction methodologies—QSSA, RCCE, and ILDM—each has advantages and disadvantages, which are summarized in Table 1. ILDM has the advantage of automatically identifying the fast directions locally in composition space. However, as the basis of a generally applicable methodology, the fact that the manifolds are not necessarily continuous appears to be an insuperable problem. These discontinuities stem from the fact that, although the Jacobian of the reaction rates varies continuously in composition space, its invariant subspaces do not. RCCE has several characteristics that suit it well to a generally applicable methodology: the maximum-entropy manifold is guaranteed to exist, to be unique, and to be continuous, and it is readily parametrized (by the chosen constraint variables).

In each of the three reduction methods, given the reduced description of the composition (in terms of n_r variables), the full composition (n variables) implied by the method is determined by solving a set of nonlinear equations. RCCE is distinguished by the fact that the nonlinear system consists of just n_r equations, rather than n or $n - n_r$ in ILDM and QSSA. This makes RCCE particularly attractive for very large mechanisms (e.g., $n = 1000$ [15]).

The structure of the paper is as follows. The mathematical descriptions of ISAT and rate-controlled constrained equilibrium are stated in the next two sections. We then present the implementation of ISAT-RCCE. The accuracy and efficiency of ISAT-RCCE are then demonstrated by making comparisons with detailed kinetic calculations. This is done for the test case of a nonpremixed pairwise mixing stirred reactors using a detailed mechanism for methane oxidation. Conclusions are drawn in the final section.

Methodology

To simplify the notation, we consider a homogeneous reactive gaseous flow, although the new methodology is generally applicable to other complex situations. The thermochemical state of the mixture is completely determined by $n_s + 2$ variables (where n_s denotes the number of species), namely, the specific mole numbers ϕ_i (moles of species i per kg of mixture), the specific enthalpy H, and the system pressure P. Thus, the state of the chemical system is given as a point in an $n(= n_s + 2)$-dimensional *composition space* Z. The evolution of the state vector $\boldsymbol{\varphi} = (\phi_1, \phi_2, \ldots, \phi_{ns}, P, H)^T$ in the space Z is described by

$$\dot{\varphi} = d\boldsymbol{\varphi}/dt = \mathbf{s}(\boldsymbol{\varphi}[t]) \qquad (1)$$

where $\mathbf{s}$ is an $n \times 1$ vector representing the rate of change due to reaction.

ISAT

For a given fixed time interval Δt, the *reaction mapping* $\mathbf{R}(\boldsymbol{\varphi})$ is defined to be the solution to equation 1 after time Δt from the initial condition $\boldsymbol{\varphi}$. In ISAT, information about $\mathbf{R}(\boldsymbol{\varphi})$ is stored at tabulation points. At the mth point, the initial composition is $\boldsymbol{\varphi}^{(m)}$, the mapping is $\mathbf{R}^{(m)} \equiv \mathbf{R}(\boldsymbol{\varphi}^{(m)})$, and the *mapping gradient* is $\mathbf{A}^{(m)} \equiv \mathbf{A}(\boldsymbol{\varphi}^{(m)})$, where

$$A_{ij}(\boldsymbol{\varphi}) \equiv \partial R_i(\boldsymbol{\varphi})/\partial \varphi_j \tag{2}$$

A linear approximation to $\mathbf{R}(\boldsymbol{\varphi})$ for points $\boldsymbol{\varphi}$ close to $\boldsymbol{\varphi}^{(m)}$ is

$$\mathbf{R}(\boldsymbol{\varphi}) \approx \hat{\mathbf{R}}^{(m)}(\boldsymbol{\varphi}) \equiv \mathbf{R}^{(m)} + \mathbf{A}^{(m)}(\boldsymbol{\varphi} - \boldsymbol{\varphi}^{(m)}) \tag{3}$$

The retrieval is based on the linear approximation equation 3, given that the error involved is less than a specified tolerance ε_{tol}. If the linear approximation is insufficiently accurate, then a table entry is added at the point $\boldsymbol{\varphi}$ by directly integrating equation 1. A complete description of ISAT can be found in Ref. [6].

RCCE

The RCCE [3,16] method is based on the assumption that the fast reactions (in a complex reacting system) cause the composition to relax to a partial equilibrium state, subject to the constraints imposed by slow reactions. Here (in addition to the pressure P and enthalpy H), we take the n_c constraints to be the specific moles of the n_e elements and of a specified set of $(n_c - n_e)$ species and/or their linear combinations. The system reaches complete equilibrium by evolving on a low-dimensional manifold of constrained equilibrium states. This n_c-dimensional constrained equilibrium manifold can be determined by maximizing the entropy subject to the values of the constraints. Thus, only the rate equations of the slowly changing constraints need be integrated, and the size of this ordinary differential equation (ODE) system (n_c) can be much smaller than the number of species (n_s). Moreover, the constrained equilibrium problem can be solved economically using the concept of Lagrange multipliers [3,16,17], where n_c constraint potentials $(\lambda_1, \lambda_2, \ldots, \lambda_{nc})$ (Lagrange multipliers conjugate to the constraints) uniquely determine all species compositions in the constrained equilibrium state.

For given pressure P and enthalpy H, the constrained equilibrium state is represented by the vector of specific mole numbers $\boldsymbol{\phi} = (\phi_1, \phi_2, \ldots, \phi_{ns})^T$ whose evolution can still be described by equation 1—replacing $\boldsymbol{\varphi}$ by $\boldsymbol{\phi}$—but only has n_c degrees of freedom. The relationships among constraints $\mathbf{c}$, constraint potentials $\boldsymbol{\lambda}$, and composition $\boldsymbol{\phi}$ are revealed in Refs. [3,17] and are presented here. The n_c constraints are

$$c_i = B_{ji}\phi_j,\ i = 1, \ldots, n_c,\ j = 1, \ldots, n_s \tag{4}$$

where B_{ji} is the value of constraint i for the species j. It is required that the constraints be linearly independent, so that the matrix $\mathbf{B}$ has full column rank. The constrained equilibrium composition can be expressed in terms of $\boldsymbol{\lambda}$ as

$$\phi_j = N \exp\{-\tilde{g}_j(P, T) + B_{jk}\lambda_k\} \tag{5}$$

where

$$N = \sum_{j=1}^{n_s} \phi_j \tag{6}$$

is the total specific numbers of mole of the mixture, and $\tilde{g}_j$ is the dimensionless standard Gibbs free energy of species j.

By differentiating equation 4 with respect to time t, and combining with equation 1, we obtain the rate equations for constraints:

$$\dot{c}_i = s_i^c, \quad i = 1, \ldots, n_c, \tag{7}$$

where

$$s_i^c \equiv B_{ji}\dot{\phi}_j = B_{ji}s_j \tag{8}$$

is a function of P, T, and $\boldsymbol{\phi}$. The dynamics of the chemical system can then be described by equation 7 in RCCE instead of equation 1.

Equivalently, the rate equations for the constraint potentials were also derived in Ref. [3]. The method which involves direct integration of the rate equations for the constraint potentials has been tested for stoichiometric mixtures of hydrogen and air in an adiabatic constant-volume chamber [16].

Implementation

We first decompose the n-dimensional $(n = n_s + 2)$ composition space Z into two subspaces: the n_r-dimensional constraint subspace X and its orthogonal complement—the unrepresented subspace Y with dimensionality $n - n_r$. Thus, the constrained equilibrium manifold can be parametrized in the subspace X, and the tabulation on this low-dimensional subspace is straightforward. In general, the ISAT algorithm can be applied to any differentiable mapping problem in the form of $\mathbf{x} \mapsto \mathbf{f}(\mathbf{x})$, while in ISAT-RCCE, $\mathbf{x}$ becomes the initial constraints vector $\mathbf{c}^0$, and $\mathbf{f}$ is the reaction mapping $\mathbf{Q}(\mathbf{c}^0)$ in the same subspace X. Rigorous definition of $\mathbf{Q}$ is given later.

Table Generation

Two basic processes are carried out in the ISAT-RCCE algorithm: the table generation (additions and growths, see Ref. [6]) and retrievals. The major task in building up the unstructured table can be defined as: given an initial point in the subspace X,

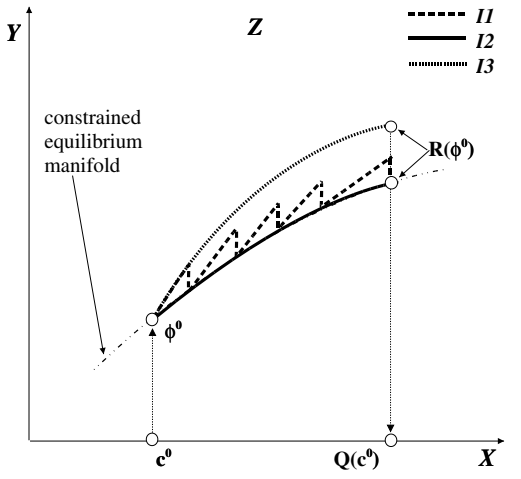

FIG. 1. Sketch for different implementations of ISAT-RCCE showing the initial point $\boldsymbol{\phi}^0$ and its reaction mapping $\mathbf{R}$ ($\boldsymbol{\phi}^0$) in the full space and in the reduced constraint space $\mathbf{c}^0$, $\mathbf{Q}(\mathbf{c}^0)$.

determine the reaction mapping in the same subspace by integrating the ODEs associated with the constrained equilibrium manifold. Traditionally in RCCE [3,18], equation 7—the rate equations of constraints—are integrated in a stepwise fashion. In our implementation, the process becomes: given the initial value $\mathbf{c}^0$ and Δt, integrate equation 7 over this time interval, and the solution is the reaction mapping $\mathbf{Q}(\mathbf{c}^0)$. We call this implementation I1. If a multistep ODE solver is used, the solution trajectory in the space Z can be portrayed as the dashed line in Fig. 1. Since the manifold is not inertial, the constrained equilibrium composition must be evaluated at each substep and the trajectory is projected back onto the manifold.

An alternative approach suggested in Ref. [3] is to integrate the rate equations for the constraint potentials. This implementation (I2) explicitly solves for $\boldsymbol{\lambda}$ and is expected to be more economical than the previous one. However, it is the constraint values that are communicated with the outside reactive flow code. So two additional pieces of work must be performed by solving equations 4–6: convert the constraints $\mathbf{c}^0$ to the initial constraint potentials $\boldsymbol{\lambda}^0$, and change $\boldsymbol{\lambda}^1$—the solution after time Δt—back to constraints, that is, to the reaction mapping $\mathbf{Q}(\mathbf{c}^0)$. The solution trajectory of this approach is drawn as the solid line in Fig. 1, which follows the manifold everywhere in space Z. It is noted that as the sub-time step δt approaches 0 in solving the equations, I1 and I2 will generate the same results and thus are fully consistent with each other.

Our current table generation process (I3) is slightly different from the above discussions and can be viewed as an approximation to I1. As shown in Fig. 1 by the dotted line, after getting the initial constrained equilibrium composition $\boldsymbol{\phi}^0$ from $\mathbf{c}^0$, we solve the entire ODEs system equation 1 over the time interval Δt, and the resulted $\mathbf{R}(\boldsymbol{\phi}^0)$ is no longer on the manifold. The required reaction mapping $\mathbf{Q}(\mathbf{c}^0)$ is simply the orthogonal projection of $\mathbf{R}$ in the Z space onto the X subspace and can be written as

$$Q_i(\mathbf{c}^0) \equiv B_{ji}R_j(\boldsymbol{\phi}^0) \tag{9}$$

I3 is easily achieved by slightly modifying the existing ISAT program, and all results presented here are generated by this approach. Nevertheless, there is no doubt that I2 is a superior approach, and its implementation is in progress.

Retrieval

The retrieval process is based on the linear approximation similar to equation 3, but in the reduced subspace X. For the mth table entry, it reads

$$\mathbf{Q}(\mathbf{c}) \approx \hat{\mathbf{Q}}^{(m)}(\mathbf{c}) \equiv \mathbf{Q}^{(m)} + \bar{\mathbf{A}}^{(m)}(\mathbf{c} - \mathbf{c}^{(m)}) \tag{10}$$

where the $n_c \times n_c$ modified mapping gradient matrix $\bar{\mathbf{A}}$ is defined as $\bar{A}_{ij}(\mathbf{c}) \equiv \partial Q_i(c)/\partial c_j$. To implement ISAT, it is necessary to have a procedure to evaluate the matrix $\bar{\mathbf{A}}$. This is straightforward whether RCCE is implemented by solving equation 7 for $\mathbf{c}$ (I1), the rate equations for $\boldsymbol{\lambda}$ (I2), or (as we do here) equation 1 for $\mathbf{R}(\boldsymbol{\phi}^0)$ and then obtaining $\mathbf{Q}(\mathbf{c})$ from equation 9 (I3).

For implementation I1, the mapping gradients $\bar{\mathbf{A}}$ are related to sensitivity coefficients. When solving equation 7, the first-order sensitivity coefficients with respect to initial conditions are defined by

$$G_{ij}(\mathbf{c}^0, t) \equiv \partial c_i(t)/\partial c_j^0 \tag{11}$$

and then the mapping gradients are

$$\bar{\mathbf{A}}(\mathbf{c}^0) = \mathbf{G}(\mathbf{c}^0, \Delta t) \tag{12}$$

It is readily deduced from equation 7 that $\mathbf{G}$ evolves according to the linear system of ordinary differential equations

$$\dot{\mathbf{G}}(\mathbf{c}^0, t) = \mathbf{J}(\mathbf{c}[t])\mathbf{G}(\mathbf{c}^0, t) \tag{13}$$

where $\mathbf{J}$ is the Jacobian $J_{ij}(\mathbf{c}) \equiv \partial s_i^c(\mathbf{c})/\partial c_j$, and the initial condition is $\mathbf{G}(\mathbf{c}^0, 0) = \mathbf{I}$. In the computational implementation of the method, equations 7 and 13 can be solved together using the DDASAC code [19] to obtain $\mathbf{Q}(\mathbf{c}^0)$ and $\bar{\mathbf{A}}(\mathbf{c}^0)$.

For I2 and I3, the gradient matrix $\bar{\mathbf{A}}$ can be expressed by chain rule as

$$\bar{A}_{ij} = \partial Q_i/\partial c_j^0 = (\partial Q_i/\partial \lambda_k^1)(\partial \lambda_k^1/\partial \lambda_l^0)(\partial \lambda_l^0/\partial c_j^0) \tag{14}$$

and

$$\bar{A}_{ij} = \partial Q_i/\partial c_j^0 = (\partial Q_i/\partial R_k)(\partial R_k/\partial \phi_l^0)(\partial \phi_l^0/\partial c_j^0) \tag{15}$$

respectively. The evaluations of the different terms in equation 15 are given in the Appendix.

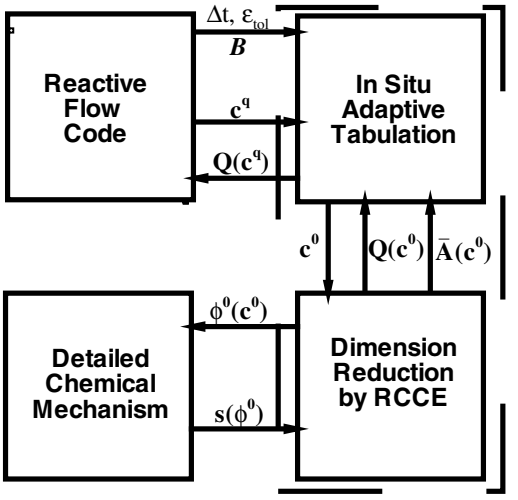

FIG. 2. Overview of the interconnection between a reactive flow code, the ISAT-RCCE algorithm, and a detailed chemistry mechanism.

Figure 2 gives an overview of the functioning of the ISAT-RCCE algorithm in terms of computer program modules. The reactive flow code initializes ISAT-RCCE by providing the time step Δt, the error tolerance ε_{tol}, and the definition of constraint subspace X (in terms of the constraint matrix $\mathbf{B}$). After that, the ISAT-RCCE can be treated as a black box—receiving query constraints $\mathbf{c}^{\text{q}}$ and returning the mapping $\mathbf{Q}(\mathbf{c}^{\text{q}})$ (to the required accuracy). The high-dimensional detailed mechanism serves as a database, which evaluates the rate of change due to reaction corresponding to the received manifold compositions.

Test Results

Pairwise Mixing Stirred Reactor Test Case

The pairwise mixing stirred reactor (PMSR) is a stringent test bed for chemistry implementation. A description of PMSR is given in Ref. [20] and briefly repeated here. At time t, the PMSR consists of a specified even number M of particles whose constraint vectors are denoted by $\mathbf{c}^{[1]}(t)$, $\mathbf{c}^{[2]}(t)$, . . . , $\mathbf{c}^{[M]}(t)$. With Δt being the specified time step, at the discrete times $k\Delta t$ (k integer) events occur corresponding to *outflow, inflow,* and *pairing.* Between these discrete times, the composition of particles evolves by a *mixing* fraction step (with τ_{mix} being the mixing time scale) and a *reaction* fraction step, in which the particles evolves by equation 7.

With τ_{res} being the specified residence time, outflow and inflow consist of selecting $\frac{1}{2}M\Delta t/\tau_{\text{res}}$ pairs at random and replacing their constraints according to inflow compositions, which are drawn from a specified distribution. With τ_{pair} being the specified pairing time scale, $\frac{1}{2}M\Delta t/\tau_{\text{pair}}$ pairs of particles (other than the inflow particles) are randomly selected for pairing.

The values of the parameters used in the PMSR calculations are chosen as the following: $M = 100$, $\Delta t = 0.1$ (ms), $\tau_{\text{res}} = 10$ (ms), and $\tau_{\text{mix}} = \tau_{\text{pair}} = 1$ (ms). Calculations are performed adiabatically with constant pressure. There are three in-flowing streams: air (79% N2, 21% O2) at 300 K; methane at 300 K; and a pilot stream consisting of an equilibrium, stoichiometric fuel/air mixture at 2595 K. The mass flow rates of these streams are in the ratio 0.85:0.05:0.1.

Performance of ISAT-RCCE

The GRI-Mech 1.2 [21] is taken to be the detailed mechanism with the total degrees of freedom of the system being 32 (number of species plus enthalpy). Three different tests (referred to as C1, C2, and C3) are performed. In C1 the constrained species are H_2O, CO_2, O_2, CH_4, and CO. Three more species (H_2, OH, and O) are added to form the constraint subspace in C2, and in C3 an additional three species (CH_3, C_2H_2, and C_2H_4) are included. Additional constraints are imposed on all four elements and enthalpy, and hence the dimension reductions are from 32 to 10, 13, and 16 for the three cases, respectively. The error tolerance ε_{tol} in ISAT is set to be 5×10^{-4}.

To test the accuracy of the algorithm, we solve the entire ODE system (32-dimensional) by direct integration (DI) to get the accurate solution. Both DI and ISAT-RCCE calculations bear the same in-flowing condition; thus a direct comparison can be made between them. Fig. 3 shows the relative error in species compositions, temperature, and density against their reference values for one particle (advanced over 2000 time steps in the statistically stationary state). It can be observed that, as the number of constraints increases, the error in the constrained species decreases. For C3, the relative errors in major species (including CO and H_2) are under 3% with the errors of other constrained species being less than 10%. For density (ρ) and temperature (T) required by the outside reactive flow code, the predictions are very good for all three cases with errors less than 2%. Large errors can be found for unrepresented species. The results show that bringing some unrepresented species into the constrained subspace effectively improves their predictions (e.g., the error of C_2H_4 changes from 150% in C2 to 9% in C3). The works in Refs. [3,16,18] suggest another possibility to improve the accuracy, which is to impose constraints on linear combinations of species instead of individual species. Investigation of this issue is a subject of future work.

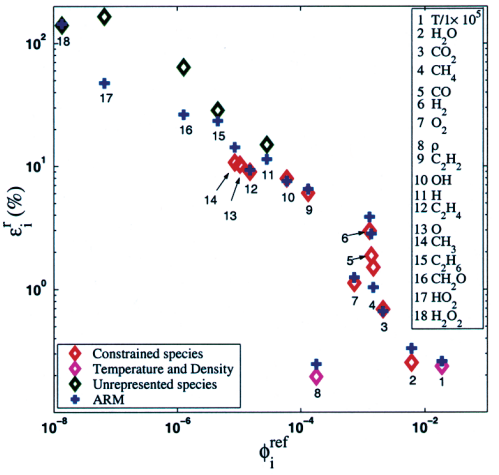

FIG. 3. Relative errors against reference values for one particle (different constraints). $\varepsilon_i^r \equiv \Sigma_t|\phi_i^{\mathrm{ISAT}}(t) - \phi_i^{\mathrm{DI}}(t)| \times 200/\Sigma_t(\phi_i^{\mathrm{ISAT}}(t) + \phi_i^{\mathrm{DI}}(t))$, where the superscript ISAT denotes the results from ISAT-RCCE and DI denotes the accurate solution. ϕ_i^{ref} is the accurate mean specific mole number of species i over time t. Constrained species, bold empty symbols; unrepresented species, normal empty symbols; density and temperature, solid symbols.

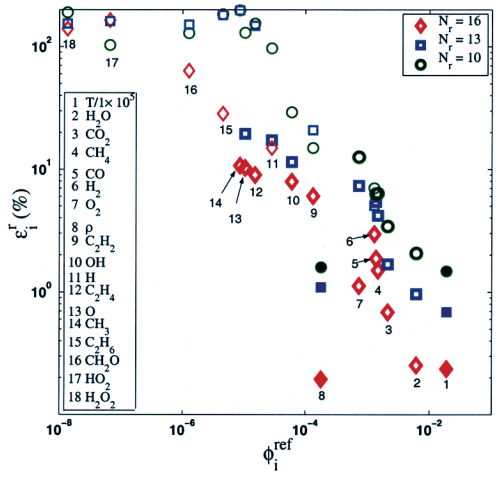

FIG. 4. Relative errors against reference values for one particle (different constraints). $\varepsilon_i^r \equiv \Sigma_t|\phi_i^{\mathrm{ISAT}}(t) - \phi_i^{\mathrm{DI}}(t)| \times 200/\Sigma_t(\phi_i^{\mathrm{ISAT}}(t) + \phi_i^{\mathrm{DI}}(t))$, where the superscript ISAT denotes the results from ISAT-RCCE or ISAT-QSSA and DI denotes the accurate solution. ϕ_i^{ref} is the accurate mean specific mole number of species i over time t.

A reference ISAT-QSSA calculation (using a 17-dimensional augmented reduced mechanism [14] derived from GRI-Mech 1.2) is also performed, and the results (see Fig. 4) show comparable accuracy to that of C3. For the species in the constrained subspace, temperature, and density, the calculation errors are at the same level for the two methods, while for those species in the unrepresented subspace of C3 but explicitly included in the reduced mechanism, the ISAT-QSSA calculation shows relatively better results, except for H_2O_2 which is not well predicted in both calculations.

The ISAT-RCCE algorithm inherits the high efficiency of ISAT. In our test case C3 (calculation for 10^5 residence times), a speed-up factor of around 500 is achieved in terms of CPU time relative to the calculation by direct integration of the full set of governing equations. With the same ISAT error tolerance, our current implementation (I3) of the ISAT-RCCE algorithm spends more CPU time in building and updating the tabulation table than the ISAT-QSSA method does. However, the total CPU times of the test calculations using the two methods are still comparable because it is the linear retrieval process that dominants the CPU time consumption in a long run. Further improvment in efficiency can be expected after implementing I2 in ISAT-RCCE.

Conclusions and Future Work

A new accurate and efficient methodology ISAT-RCCE is developed to incorporate combustion chemistry in reacting flow modeling. The test results (C3) from the new method are in good agreement with the accurate solution (less than 3% error for density, temperature, and major species including CO and H_2), which is comparable to an ISAT-QSSA calculation with a similar level of dimension reduction (32 to 17). A speed-up factor of around 500 (in C3) is obtained compared to the direct integration approach and is also comparable to that of the ISAT-QSSA method.

In future work, a more consistent and economic implementation (I2) of ISAT-RCCE will be developed as well as the methodology to choose the optimal constrained subspace, and the application of this method in practical combustion calculations is expected.

Appendix

Equation 15 can be written in matrix form

$$\bar{\mathbf{A}} = \mathbf{B}^{\mathbf{T}}\,\mathbf{A}\,\mathbf{T} \tag{16}$$

where $B_{ki} \equiv \partial Q_i/\partial R_k$ is the constraints matrix in equation 9; $\mathbf{A}$ is defined in equation 2 and can be calculated by DDASAC while solving equation 1 in

I1. The $n_s \times n_c$ matrix $\mathbf{T}$ is defined as $T_{ij} \equiv \partial\phi_i/\partial c_j$. It should be pointed out that the column vectors of $\mathbf{T}$ span the tangent plane of the constrained equilibrium manifold at point $\mathbf{c}$ and they can be evaluated analytically through $\boldsymbol{\lambda}$.

For simplicity, we derive the expression for $\mathbf{T}$ at constant temperature and pressure such that the Gibbs free energy $\tilde{\mathbf{g}}$ is fixed. Let us first differentiate equation 5 with respect to the constraint $\mathbf{c}$

$$\partial\phi_j/\partial c_k = \phi_j\, \partial\, \ln\{N\}/\partial c_k + \phi_j B_{(j)i}\partial\lambda_i/\partial c_k \quad (17)$$

Then we differentiate equation 4 (written for c_l) and substitute equation 17 to obtain

$$\delta_{lk} = B_{jl}\, \partial\phi_j/\partial c_k = c_l\, \partial\, \ln\{N\}/\partial c_k + D_{li}\, \partial\lambda_i/\partial c_k \quad (18)$$

with $D_{li} = B_{kl}\phi_k B_{(k)i}$. Summing equation 17 over $j = 1, \ldots, n_s$, we obtain

$$\sum_{j=1}^{n_s}\partial\phi_j/\partial c_k = \partial N/\partial c_k = \partial N/\partial c_k + \sum_{j=1}^{n_s}\phi_j B_{(j)i}\partial\lambda_i/\partial c_k \quad (19)$$

and thus

$$\sum_{j=1}^{n_s}\phi_j B_{(j)i}\, \partial\lambda_i/\partial c_k = c_i\, \partial\lambda_i/\partial c_k = 0 \quad (20)$$

By manipulating equations 17, 18, and 20, the matrix $\mathbf{T}$ can be expressed as

$$\mathbf{T} = \boldsymbol{\phi}\boldsymbol{\mu} + \mathbf{U} \quad (21)$$

with $\mu_i \equiv \partial\, \ln\{N\}/\partial c_i$, $U_{ji} \equiv \phi_j B_{(j)k} L_{ki}$, and $L_{ik} \equiv \partial\lambda_i/\partial c_k$. The $1 \times n_c$ vector $\boldsymbol{\mu}$ and the $n_c \times n_c$ matrix $\mathbf{L}$ can be computed by

$$\boldsymbol{\mu} = (\mathbf{c}^T\mathbf{D}^{-1})/(\mathbf{c}^T\mathbf{D}^{-1}\mathbf{c})$$
$$\mathbf{L} = \mathbf{D}^{-1} - (\mathbf{D}^{-1}\mathbf{c}\mathbf{c}^T\mathbf{D}^{-1})/(\mathbf{c}^T\mathbf{D}^{-1}\mathbf{c}) \quad (22)$$

Thus, given the constraint $\mathbf{c}$ and the corresponding equilibrium composition $\boldsymbol{\phi}$, the tangent plane of the manifold is known. The matrix $\mathbf{D}$ must be nonsingular at every point on the manifold for equation 22 to be well posed. It is easy to show that sufficient conditions for $\mathbf{D}$ to be non-singular are that the constraints be linearly independent and that the species-specific moles be strictly positive.

Acknowledgment

This work is supported by Air Force Scientific Office of Research grant F-49620-00-1-0171.

REFERENCES

1. Smooke, M. D., (ed.), "Reduced Kinetic Mechanisms and Asymptotic Approximations for Methane-Air Flames," *Lecture Notes in Physics, Vol. 384*, Springer, Berlin, 1991.
2. Lam, S. H., and Goussis, D. A., *Proc. Combust. Inst.* 22:931 (1988).
3. Keck, J. C., *Prog. Energy Combust. Sci.* 16:125 (1990).
4. Mass, U., and Pope, S. B., *Combust. Flame* 88:239 (1992).
5. Chen, J.-Y., Kollmann, W., and Dibble, R. W., *Combust. Sci. Technol.* 64:315 (1989).
6. Pope, S. B., *Combust. Theory Modelling* 1:41 (1997).
7. Turányi, T., *Comput. Chem.* 18:45 (1994).
8. Tonse, S. R., Moriarty, N. W., Brown, N. J., and Frenklach, M., *Isr. J. Chem.* 39(1):97 (1999).
9. Christo, F. C., Masri, A. R., and Nebot, E. M., *Combust. Flame* 106:406 (1996).
10. Rabitz, H., and Aliş, Ö., *J. Math. Chem.* 25:197 (1999).
11. Xu, J., and Pope, S. B., *Combust. Flame* 123:281 (2000).
12. Tang, Q., Xu, J., and Pope, S. B., *Proc. Combust. Inst.* 28:133 (2000).
13. James, S., Anand, M. S., Razdan, M. K., and Pope, S. B., *ASME J. Eng. Gas Turb. Power* 123:747 (2001).
14. Sung, C. J., Law, C. K., and Chen, J. Y., *Combust. Flame* 125(1–2):906 (2001).
15. Warnatz, J., *Proc. Combust. Inst.* 24:553 (1992).
16. Hamiroune, D., Bishnu, P., Metghalchi, M., and Keck, J. C., *Combust. Theory Modelling* 2:81 (1998).
17. Reynolds, W. C., *The Element Potential Method for Chemical Equilibrium Analysis: Implementation in the Interactive Program STANJAN*, Mechanical Engineering Department, Stanford University, Stanford, CA, 1986.
18. Yousefian, V., *Combust. Flame* 115:66 (1998).
19. Caracotsios, M., and Stewart, W. E., *Comput. Chem. Eng.* 9(4):359 (1985).
20. Yang, B., and Pope, S. B., *Combust. Flame* 112:16 (1998).
21. Frenklach, M., Wang, H., Goldenberg, M., Smith, G. P., Golden, D. M., Bowman, C. T., Hanson, R. K., Gardiner, W. C., and Lissianski, V., *GRI-Mech: An Optimized Detailed Chemical Reaction Mechanism for Methane Combustion,* Gas Research Institute topical report, Gas Research Institute, Chicago, 1995.